JCI insight

RESEARCH ARTICLE

IL-7–dependent STAT1 activation limits homeostatic CD4+ T cell expansion

Cecile Le Saout,[1] Megan A. Luckey,[2] Alejandro V. Villarino,[3] Mindy Smith,[1] Rebecca B. Hasley,[1] Timothy G. Myers,[4] Hiromi Imamichi,[1] Jung-Hyun Park,[2] John J. O'Shea,[3] H. Clifford Lane,[1] and Marta Catalfamo[1,5]

[1]CMRS/Laboratory of Immunoregulation, NIAID, [2]Experimental Immunology Branch, CCR, NCI, [3]Lymphocyte Cell Biology Section, NIAMS, and [4]Genomic Technologies Section, Research Technologies Branch, NIAID, NIH, Bethesda, Maryland, USA. [5]Department of Microbiology and Immunology, Georgetown University School of Medicine, Washington, DC, USA

IL-7 regulates homeostatic mechanisms that maintain the overall size of the T cell pool throughout life. We show that, under steady-state conditions, IL-7 signaling is principally mediated by activation of signal transducers and activators of transcription 5 (STAT5). In contrast, under lymphopenic conditions, there is a modulation of STAT1 expression resulting in an IL-7–dependent STAT1 and STAT5 activation. Consequently, the IL-7–induced transcriptome is altered with enrichment of IFN-stimulated genes (ISGs). Moreover, STAT1 overexpression was associated with reduced survival in CD4+ T cells undergoing lymphopenia-induced proliferation (LIP). We propose a model in which T cells undergoing LIP upregulate STAT1 protein, "switching on" an alternate IL-7–dependent program. This mechanism could be a physiological process to regulate the expansion and size of the CD4+ T cell pool. During HIV infection, the virus could exploit this pathway, leading to the homeostatic dysregulation of the T cell pools observed in these patients.

Introduction

T cell homeostasis is a mechanism designed to preserve the diversity of the T cell repertoire throughout life (1, 2). This is achieved by balancing survival and proliferation signals provided by T cell receptor (TCR) engagement to self-peptide–MHC complexes and homeostatic cytokines such as IL-7 and IL-15 (3–8). IL-7 is a critical factor for naive CD4+ and CD8+ T cell homeostasis, and in immune deficient hosts, it supports Lymphopenia-induced proliferation (LIP) (9, 10). In these conditions, CD8+ T cells undergo greater proliferation than CD4+ T cells, leading to the hypothesis that these 2 pools may have distinct sensitivity to homeostatic cytokines, and/or intrinsic features of these pools may contribute to explain these differences (11, 12).

In human lymphopenic conditions such as HIV infection and BM transplants, there is an increased availability of IL-7 (13–15). Particularly, in patients with HIV infection, the CD4+ T cell pool is under constant homeostatic pressure because of its depletion. This effect is evident by the negative correlation between the rate of proliferating CD4+ T cells and CD4+ T cell counts. A similar relationship is observed in healthy volunteers (16). In contrast, such a correlation is not observed in the CD8+ T cell pool from patients and healthy volunteers. In patients with HIV infection, following combination antiretroviral therapy (cART), the CD4+ T cell reconstitution is slow and could take many years, depending on the CD4+ T cell number prior to initiation of therapy (17–19). Together, these observations suggest that CD4+ and CD8+ T cell pools are differentially regulated and these characteristics may be exploited by HIV, contributing to the dysregulation of the T cell pools observed in these patients (16, 20–24).

IL-7 signals through a heterodimer receptor composed of the IL-7Rα and the γc chains, which are respectively associated to Janus kinase-1 (JAK1) and JAK3 (25, 26). Binding of IL-7 to its heterodimer receptor leads to transphosphorylation of JAK1 and JAK3. The phosphorylated active form of JAK3 then phosphorylates tyrosine 449 on IL-7Rα, generating a docking site for the signal transducers and activators of transcription 5 (STAT5). The phosphorylated heterodimers STAT5a and STAT5b translocate to the nucleus and initiate transcription of target genes (27–29). In addition to the JAK/STAT pathway, IL-7/IL-7R signaling induces activation of phosphoinositide 3-kinase (PI[3]K)/AKT pathway (30, 31).

In this study, we present evidence that, in T cells undergoing LIP, IL-7 modulates the expression levels of STAT1 protein, resulting in IL-7–dependent STAT1 and STAT5 signaling. We undertook this study to

Conflict of interest: The authors have declared that no conflict of interest exists.

Submitted: July 12, 2017
Accepted: October 11, 2017
Published: November 16, 2017

Reference information:
JCI Insight. 2017;2(22):e96228.
https://doi.org/10.1172/jci.insight.96228.

understand the contribution of IL-7–dependent STAT1 activation on T cell homeostasis in the setting of lymphopenia. Further, we identified the potential involvement of this pathway in the dysregulation of the T cells pools observed in HIV-infected patients.

Results

IL-7 induces expression and activation of STAT1. Cytokines signal through STATs, and the modulation of the expression levels of these transcription factors may induce qualitative changes in the T cell response to cytokines (32, 33). IL-7 is reported to signal primarily through STAT5. However, several reports have also shown its ability to activate STAT1, although this pathway is not well characterized (34–36). We found that IL-7 in vitro can modulate the expression levels of STAT1 protein, which we will refer to as total STAT1 protein (t-STAT1), to distinguish it from the activated phosphorylated form, p-STAT1 (37). We hypothesized that upregulation of t-STAT1 may induce changes in the usage of STATs when T cells respond to IL-7. To this end, we induced upregulation of t-STAT1 in $CD4^+$ T cells by in vitro culture with recombinant human IL-7 (rhIL-7) (Figure 1A). High levels of t-STAT1 led to p-STAT1, in addition to the canonical STAT5 (p-STAT5) (Figure 1A). These results suggest that in vivo in the settings of lymphopenia, where IL-7 levels are increased, IL-7 could signal through STAT1 and STAT5.

Because of the potential relevance of these observations in human disease such as HIV infection, we hypothesized that this pathway may be active in patients with HIV infection, in whom the $CD4^+$ T cell pool is in constant homeostatic pressure as result of its depletion. To rule out if this pathway could represent a physiological mechanism or was specific for HIV infection, we studied a cohort of HIV-infected patients ($n = 53$) receiving cART and suppressed viremia to < 50 copies/ml for more than 9 months. HIV-infected patients and healthy controls had normal range values of lymphocyte and T lymphocyte counts. Patients with HIV infection had a degree of $CD4^+$ T cell depletion, with $CD4^+$ T cell counts ranging from an interquartile range (IQR) of 148–1,001 cells/μl and median $CD4^+/CD8^+$ T cell ratio of 0.51 (IQR: 0.24–0.98) (Table 1). In addition, we compared the HIV-infected patients with a cohort of healthy volunteers ($n = 22$) who had CD4 counts of IQR 517–1,006 (Table 1). By flow cytometry, we assessed the in vitro response to IL-7 and found a positive association between expression of t-STAT1 and activation (p-STAT1) levels in both $CD4^+$ and $CD8^+$ T cells from HIV-infected patients ($r = 0.48$, $P < 0.01$ and $r = 0.49$, $P < 0.01$, respectively) (Figure 1B). Similarly, this association was also noted for $CD4^+$ and $CD8^+$ T pools from healthy controls ($r = 0.80$, $P < 0.01$ and $r = 0.52$, $P < 0.01$, respectively) (Figure 1B). These data suggest that IL-7 signaling could use STAT1 in addition to the canonical STAT5 in the context of high STAT1 protein expression.

Lymphopenia induces IL-7–dependent STAT1 activation. To ascertain the in vivo relevance of our in vitro findings, we used a murine model of lymphopenia in which T cells adoptively transferred into $RAG^{-/-}$ undergo LIP. In this model, T cells show an IL-7–dependent slow proliferation (SP, CellTrace Violet–positive [CTV^+] cells) and a fast proliferation (FP, CTV^- cells) driven by the combination of IL-7 signals and endogenous antigens (3, 38, 39). Slow proliferating T cells showed upregulation of t-STAT1, which was not observed on T cells transferred into immune-competent B6 hosts (Figure 2A). Under these conditions, in vitro stimulation with IL-7 led to an approximately 4- and 3-fold increase in STAT1 activation in $CD4^+$ and $CD8^+$ T cells, respectively, with only 1.6-fold increase in STAT5 activation (Figure 2B). In contrast, donor T cells undergoing FP showed minimal changes in the phosphorylated form of STAT1 and STAT5 compared with donor T cells transferred into immune-competent B6 hosts (Figure 2B). These results suggest that, under steady-state conditions in an immune competent host, IL-7 signaling is mainly mediated by STAT5 phosphorylation with marginal contribution of STAT1. In contrast, upregulation of t-STAT1 under lymphopenic conditions induces alternation in IL-7 signaling, such that STAT1 signaling is employed to greater extent.

IL-7 induces a set of STAT1/IFN-associated genes in naive T cells. To explore this IL-7 signaling pathway, we next assessed the transcriptional changes induced by IL-7 in WT naive T cells. After 90 minutes of in vitro stimulation with IL-7, the vast majority of differentially expressed genes (DEGs) observed in WT $CD4^+$ naive T cells were also observed in $CD8^+$ naive T cells ($n = 632$ and $n = 622$, respectively, with 405 genes common to both) (Figure 3A). The pathway analysis of the IL-7–regulated genes, as expected, showed the γc cytokines as putative regulators in both $CD4^+$ and $CD8^+$ T cells. IL-2, IL-4, IL-7, IL-15, and the signaling molecule STAT5A were observed in the top-scoring upstream regulators predicted based on the DEGs in T cells stimulated with IL-7 (Figure 3B). Interestingly, STAT1, IFNG, IRF7, and IFNA were also noted among the top 15 best-scoring upstream regulators (Figure 3B). To analyze the potential contribu-

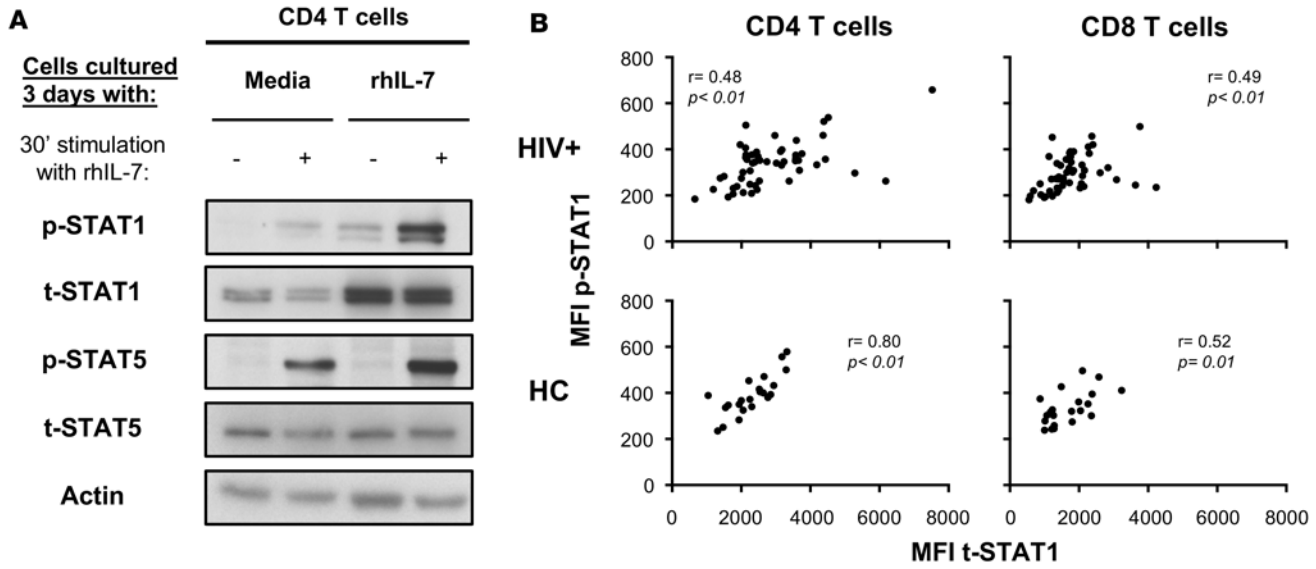

Figure 1. Increased STAT1 expression is associated with IL-7–dependent STAT1 phosphorylation. (**A**) Isolated CD4$^+$ T cells from a healthy donor were cultured 3 days in media alone or rhIL-7 (10 ng/ml). After 3 days of culture, the cells were harvested, washed, and rested overnight to allow IL-7R reexpression (52). Rested cells were then stimulated in vitro with rhIL-7 (1 ng/ml) for 30 minutes, and cell lysates were analyzed by Western blotting with antibodies specific to p-STAT1, t-STAT1, p-STAT5, and t-STAT5. An antibody to actin was used to confirm even protein loading. Results are representative of at least 3 different donors. (**B**) PBMCs from healthy controls (HC, n = 22) and HIV-infected patients with viremia suppressed to < 50 copies/ml for median 17 months on cART (HIV+, n = 53) were analyzed for t-STAT1 and p-STAT1 levels in total CD4$^+$ and CD8$^+$ T cell populations. The relationship between the STAT1 phosphorylation after 30 minutes in vitro stimulation with rhIL-7 and t-STAT1 levels was assessed using a nonparametric Spearman test.

tion of IL-7–dependent STAT1 activation, we next compared the genes regulated upon IFN-γ stimulation (STAT1-dependent) (33). A direct comparison of the sets of DEGs for IL-7 and IFN-γ stimulation revealed a relatively small overlap in CD4$^+$ and CD8$^+$ naive T cells (n = 63 and n = 70 genes, respectively) (Figure 3C, Table 2 and Supplemental Table 1; supplemental material available online with this article; https://doi.org/10.1172/jci.insight.96228DS1). The pathway analysis of the IFN-γ–stimulated WT T cells implicated, as expected, STAT1, IFNG, IFNA2, IFNB1 and IRFs as top upstream regulators (Supplemental Table 2). Interestingly, the set of DEGs observed in T cells upon IL-7 stimulation but, according to the IPA database, controlled by the upstream regulator IFNG included similar set of genes to that observed in WT T cells stimulated with IFN-γ (Supplemental Table 3). Similar observations were noted when upstream regulator STAT1 was analyzed (Supplemental Table 4). The results that implicated both IFNG and IL-7 as upstream regulators were consistent with the list of overlapping DEGs by IL-7– and IFN-γ–stimulated T cells (Figure 3C and Table 2 and Supplemental Table 1). These data suggest that IL-7, in steady-state conditions, induces a set STAT1/IFN associated genes in both CD4$^+$ and CD8$^+$ naive T cells.

Overexpression of STAT1 leads to an enrichment of STAT1/IFN genes in T cells stimulated with IL-7. We hypothesized that STAT1 overexpression leads to an enrichment of STAT1/IFN-dependent genes. To analyzed the impact of this pathway in IL-7 signaling, we generated a Tg mouse expressing the murine STAT1 protein under control of the human CD2 promoter (STAT1 Tg, Supplemental Figure 1A). STAT1 Tg mice expressed almost double t-STAT1 protein levels compared with WT littermates in both CD4$^+$ and CD8$^+$ T cells. As expected, B cells expressed similar levels of t-STAT1 in both STAT1 Tg and WT mice (Figure 4A). The overexpression of t-STAT1 in T cells did not affect total cellularity in lymphoid organs (Supplemental Figure 1B) nor absolute numbers of CD4$^+$ and CD8$^+$ T cells in the lymph nodes (LNs) (Supplemental Figure 1C). Moreover, CD4$^+$ and CD8$^+$ T cells from STAT1 Tg mice showed similar percentages of naive, central memory, and effector/effector memory cells in the LNs as their WT counterparts (Supplemental Figure 1D).

The analysis of IL-7Rα in WT and STAT1 Tg mice showed similar expression in peripheral mature CD4$^+$ and CD8$^+$ T cells (Supplemental Figure 1E). Under steady-state conditions, in vitro stimulation with IL-7 in both WT and STAT1 Tg mice led to IL-7–dependent phosphorylation of STAT1 that was significantly increased in the latter. Similar levels of STAT5 activation were observed in both strains (Figure 4B). In addition, compared with WT cells, STAT1 Tg T cells showed similar p-STAT1 levels in response

Table 1. Characteristics of cross-sectional data participants

	HIV⁺ patients (*n* = 53)	Healthy controls (*n* = 22)
HIV RNA (copies/ml)	<50	-
HIV RNA < 50 copies/ml (months)	17 (9–35)	-
Lymphocyte count (cells/μl)	2,017 (1,414–2,574)	1,554 (1,088–2,284)
CD3 count (cells/μl)	1,488 (953–2,094)	1,157 (736–1,775)
CD4 count (cells/μl)	432 (148–1,001)	689 (517–1,006)
CD8 count (cells/μl)	960 (647–1,215)	372 (197–575)
Ratio CD4/CD8 counts	0.51 (0.24–0.98)	1.67 (1.36–2.82)

Values are presented as median (interquartile range [IQR]).

to in vitro stimulation with IFN-γ, and an increased was observed upon stimulation with IFN-α (Supplemental Figure 1F). These results suggest that, in steady-state conditions, T cells from STAT1 Tg mice exhibit an increased contribution of STAT1 signaling upon IL-7 stimulation.

To assess the downstream consequences of IL-7–driven STAT1 activation, we compared the transcriptomes of WT and STAT1 Tg T cells following exposure to IL-7.

The vast majority of DEGs for IL-7 observed in WT cells were also observed in STAT1 Tg T cells (n = 508 and n = 478 common genes in CD4⁺ and CD8⁺ T cells, respectively, with 340 genes common to all) (Supplemental Figure 2A). Similar observations were noted in the DEGs after stimulation with IFN-γ (n = 164 and n = 130 common genes between WT and STAT1 Tg CD4⁺ and CD8⁺ T cells, respectively) (Supplemental Figure 2A). The pathway analysis of the IL-7–regulated genes in STAT1 Tg T cells implicated STAT1, IFNG, IRF7, and IFNA in addition to γc cytokines as top upstream regulators (Supplemental Table 5). The direct comparison of the sets of DEGs modulated by IL-7 and IFN-γ stimulation revealed a small overlap in CD4⁺ (n = 65 genes) and CD8⁺ naive T cells (n = 72 genes) (Supplemental Figure 2B).

Based on the list of DEGs in WT cells stimulated with IFN-γ, in order to exclude potential differences in the response to IFN-γ by STAT1 Tg cells, we defined an IFN signature for CD4⁺ and CD8⁺ T cells (n = 177 and n = 139, respectively). The Gene Set Enrichment Analysis (GSEA) showed an increased representation of IFN signature in STAT1 Tg compared with WT T cells with normalized enrichment scores (NES) of 2.49 and 2.81 for CD4⁺ and CD8⁺ STAT1 Tg T cells, respectively (Figure 4C). The leading edge genes in the STAT1 Tg mice included, among others, the IFN inducible GTPases such as the guanylate-binding protein family (GBPs), *Gbp 2*, *Gbp6_2*, *Gbp3*, *Gbp5*, *Gbp6*, and *Gbp10*. In addition, the immunity related GTPases (IRG) protein family was also upregulated (*Irgm1*, *Irgm2*, *Iigp1*, *Igtp*, *Tgtp1*, and *Tgtp2*). These results suggest that, in the context of higher expression levels of STAT1, IL-7–dependent STAT1 and STAT5 signaling pathways lead to the increased induction of IFN-dependent genes.

The analysis of the top 10 enriched biological processes within the DEGs unique to CD4⁺ and CD8⁺ naive T cells showed that CD4⁺ T cells in vitro stimulated with IL-7 were enriched in biological processes associated to proliferation and cell death, which were not present in the CD8⁺ T cells (Supplemental Table 6).

We next analyzed the indirect effects of the IL-7–dependent STAT1 activation upon overnight exposure to IL-7 and compared them with those induced by IFN-γ in WT CD4⁺ naive T cells. IL-7 induced a total of 2,393 genes commonly modulated in both WT and STAT1 Tg mice (Supplemental Figure 3A). In addition, stimulation with IL-7 showed 2,290 (WT mice) and 2,374 (STAT1 Tg mice) genes that were common to those induced by stimulation with IFN-γ (Supplemental Figure 3B and Supplemental Table 7).

Validation of the RNA sequencing (RNA-Seq) results was performed by quantitative PCR (qPCR) of selected genes downstream IL-7 and IFN-γ signaling. *Bcl2*, *Cish*, and *Socs2* were upregulated in CD4⁺ T cells stimulated with IL-7 but not IFN-γ, and higher upregulation of *Cish* and *Socs2* was observed in STAT1 Tg compared with WT cells (Supplemental Figure 3C). In contrast, *Cxcl10* and *Ifit1* were upregulated exclusively in response to IFN-γ. STAT1 Tg T cells showed a small although significant increase of *Ifit1* when compared with WT cells (Supplemental Figure 3C). *Socs1*, *Bik*, and *Ifi27* were upregulated in response to both IL-7 and IFN-γ. STAT1 Tg CD4⁺ T cells showed a higher trend of upregulation of these genes by both cytokines compared with WT cells (Supplemental Figure 3C). The analysis of the mostly affected categories of diseases and biological functions (Ingenuity Pathway Analysis [IPA]; www.qiagen.com/ingenuity) within DEGs in CD4⁺ naive T cells stimulated with IL-7 for 90 minutes revealed contrasting differences

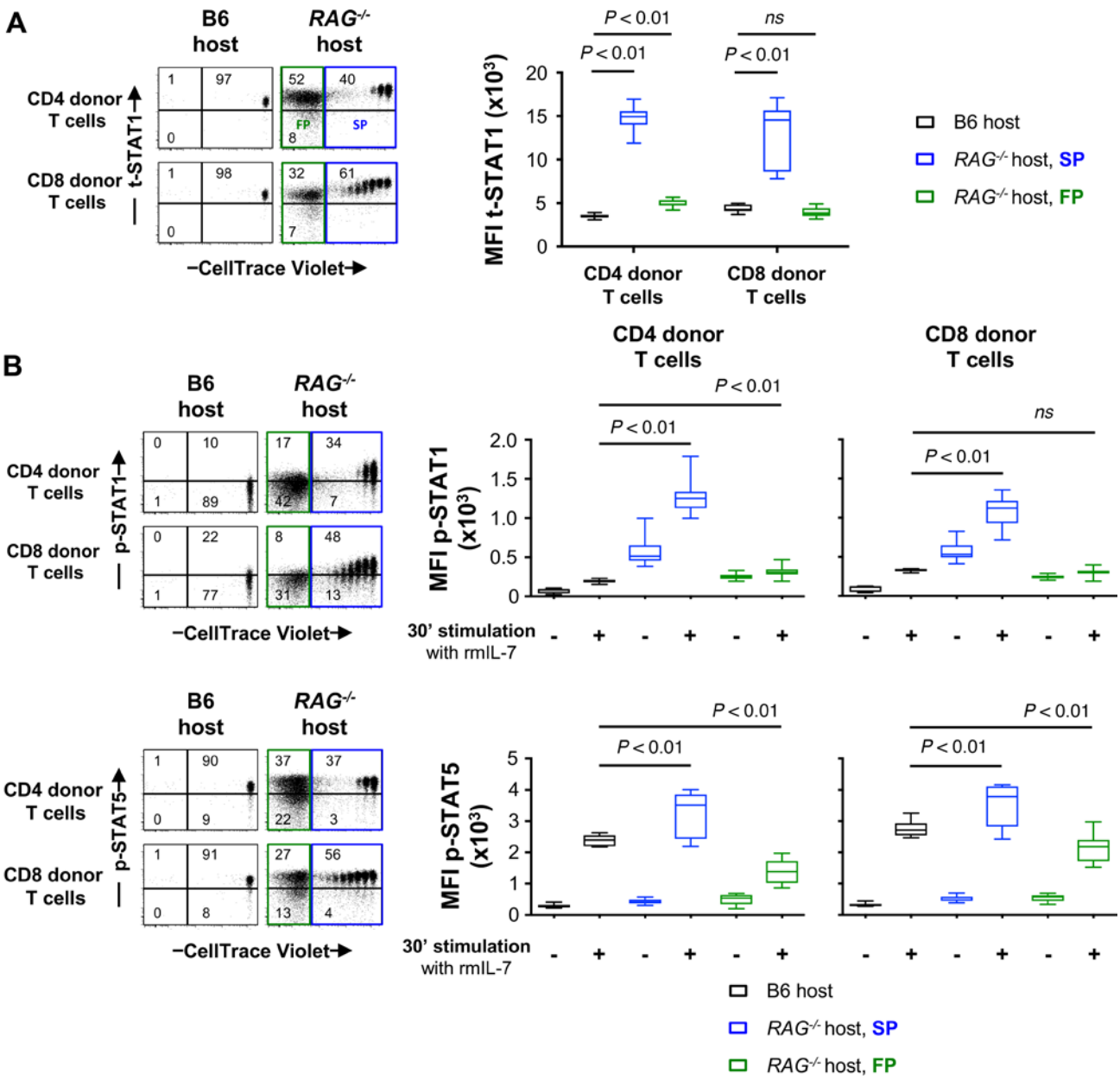

Figure 2. Lymphopenia-induced STAT1 upregulation in T cells leads to activation of STAT1 and STAT5 in response to IL-7. Lymphoreplete B6 CD45.1 (B6 host, $n = 7$) and lymphopenic *RAG*$^{-/-}$ CD45.1 (*RAG*$^{-/-}$ host, $n = 11$) mice were injected i.v. with 10×10^6 of CellTrace Violet–labeled (CTV-labeled) lymph node (LN) cells from congenic B6 CD45.2 mice. Analysis of transferred cells was performed on day 7 after transfer. The expression levels of STAT1 and activated p-STAT1 and p-STAT5 of donor T cells were evaluated by flow cytometry in LNs as function of CTV fluorescence after in vitro stimulation with rmIL-7 (1 ng/ml). Donor T cells undergoing slow proliferation (SP, CTV$^+$ cells gated in blue) and fast proliferation (FP, CTV$^-$ cells gated in green) after transfer into *RAG*$^{-/-}$ hosts were analyzed separately. (**A**) The percentages of donor T cells CTV$^+$ t-STAT1^{high}, CTV$^-$ t-STAT1^{high}, and CTV$^-$ t-STAT1^{low} are indicated. The MFIs of t-STAT1 in CD4$^+$ and CD8$^+$ donor T cells 7 days after adoptive transfer into lymphoreplete B6 (black symbols) and lymphopenic *RAG*$^{-/-}$ hosts undergoing SP (blue symbols) or FP (green symbols) were compared using a nonparametric Mann-Whitney test. (**B**) The percentages of donor T cells CTV$^+$ p-STAT1^{high}, CTV$^+$ p-STAT1^{low}, CTV$^-$ p-STAT1^{high}, and CTV$^-$ p-STAT1^{low} and CTV$^+$ p-STAT5^{high}, CTV$^+$ p-STAT5^{low}, CTV$^-$ p-STAT5^{high}, and CTV$^-$ p-STAT5^{low} are indicated. The MFIs of p-STAT1 and p-STAT5 in CD4$^+$ and CD8$^+$ donor T cells after adoptive transfer into lymphoreplete B6 (black symbols) and lymphopenic RAG$^{-/-}$ hosts undergoing SP (blue symbols) or FP (green symbols) were compared using a nonparametric Mann-Whitney test. Data are presented as box and whisker plots showing the median MFI value bounded by the first and third quartiles in the box, with whiskers extending to the minimum and maximum values, from 3 independent experiments out of 3, including an average of 2–4 mice per group per experiment.

between the STAT1 Tg and the WT cells in the pathways predicted to be activated, particularly those categories associated with cell survival and proliferation (Supplemental Figure 4A, Table 3, Table 4, and Supplemental Table 8). The analysis of diseases or functions annotations such as, "cell death" and "survival", predicted similar activation pathways in both the STAT1 Tg T cells and WT T cells (Supplemental Figure

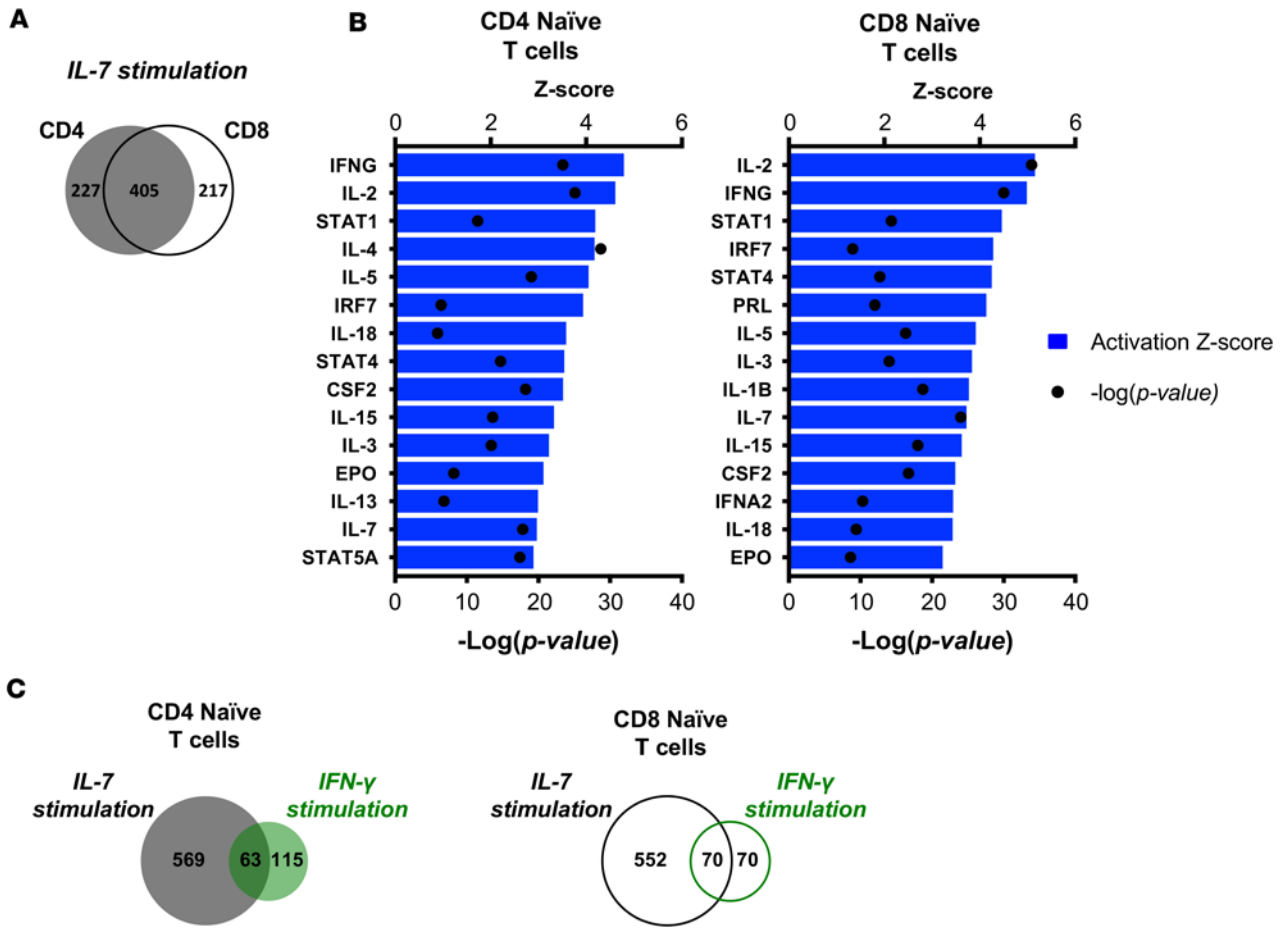

Figure 3. In vitro stimulation with IL-7 leads to activation of STAT1/IFN-regulated genes in naive T cells. Sorted WT CD4$^+$ (n = 5) and CD8$^+$ (n = 6) naive T cells were in vitro stimulated or not for 90 minutes with rmIL-7 (10 ng/ml) or rmIFN-γ (10 ng/ml). RNA was isolated and gene expression was measured by RNA-Seq. Lists of differentially expressed gene transcripts (DEGs) by IL-7 or IFN-γ stimulation in WT were selected based on gene expression changes of at least 2-fold compared with unstimulated cells. An IFN signature was defined based on the list of DEGs in WT stimulated with IFN-γ. (**A**) Venn diagram illustrates the overlap of DEGs between WT CD4$^+$ and CD8$^+$ T cells in response to IL-7. (**B**) Bar graphs show the top 15 activated upstream regulators predicted by IPA analysis in theses conditions (all predicted activators shown are significant (P <0.05). (**C**) Venn diagrams illustrate the overlap between the DEGs in WT T cells stimulated with IFN-γ (green) and IL-7 (black).

4B). In contrast, the "cell growth" and "proliferation and hematological system development and function" annotations showed an enrichment of proliferation and differentiation pathways in the WT compared with the STAT1 Tg T cells. These results suggest that STAT1-overexpressing T cells are set in a distinct transcriptional program early after IL-7 stimulation (Supplemental Figure 4B).

In contrast to the early changes observed by IL-7 stimulation, overnight culture reveals a proapoptotic potential of IL-7, which was increased in STAT1 Tg T cells (Supplemental Figure 4, C and D, Table 3, Table 4, and Supplemental Table 8).

These data show that IL-7 signaling induces STAT1/IFN-dependent genes in CD4$^+$ and CD8$^+$ T cells. In addition, in the condition of increased expression of t-STAT1 such as lymphopenia, IL-7 signaling leads to an enriched transcription of those STAT1/IFN-dependent genes, which if sustained could impact T cell survival.

STAT1 overexpression in T cells leads to impaired CD4$^+$ T cell reconstitution under lymphopenic conditions. To get insight on the biological impact of the IL-7–dependent STAT1/STAT5 signaling pathway during lymphopenic conditions in vivo, we performed adoptive T cell transfer experiments. Lymphopenic *RAG*$^{-/-}$ mice received CTV-labeled T cells from congenic WT or STAT1 Tg mice. Analysis of CTV profiles of CD4$^+$ and CD8$^+$ donor T cells at day 7 after transfer showed extensive proliferation in LNs with a small, although significant, increase in the proportion of SP STAT1 Tg T cells (Figure 5A). Nevertheless, compared with the baseline expression before the adoptive transfer into lymphopenic *RAG*$^{-/-}$ mice, both WT and STAT1 Tg donor T cells undergoing SP expressed increased STAT1 levels; however, STAT1 Tg T cells showed significantly

Table 2. Top 20 overlapping DEGs by IL-7 and IFN-γ stimulation in WT T cells

	IL-7 stimulation		IFN-γ stimulation	
Gene ID	**Log_2 (FC)[A]**	**Adjusted *P* value**	**Log_2 (FC)**	**Adjusted *P* value**
$CD4^+$ naive T cells				
Acvr1c	5.24	3.09×10^{-16}	2.77	9.28×10^{-8}
Bcl3	2.41	5.19×10^{-11}	2.88	5.54×10^{-13}
Gadd45g	3.82	1.37×10^{-9}	2.67	1.62×10^{-5}
Gata1	2.50	1.48×10^{-6}	3.94	5.46×10^{-11}
Gbp10	2.92	1.37×10^{-6}	6.65	3.01×10^{-16}
Gbp11_1	6.05	1.62×10^{-19}	4.94	2.28×10^{-16}
Gbp5	2.41	4.13×10^{-11}	4.82	4.24×10^{-21}
Gbp6_1	2.64	3.42×10^{-5}	5.48	2.24×10^{-12}
Ifi47	3.34	7.44×10^{-11}	4.79	1.69×10^{-15}
Igtp	2.64	2.03×10^{-16}	5.15	3.73×10^{-27}
Iigp1	2.68	1.89×10^{-10}	6.61	1.10×10^{-23}
Il12rb2	4.42	1.99×10^{-6}	2.51	2.71×10^{-2}
Il18rap	2.89	2.09×10^{-11}	2.61	8.02×10^{-10}
Irf4	2.25	2.76×10^{-06}	4.35	2.72×10^{-13}
Jun	2.02	4.89×10^{-10}	2.34	1.99×10^{-11}
Kit	2.02	8.39×10^{-7}	2.22	3.81×10^{-7}
Pim2	3.03	9.26×10^{-29}	2.99	1.52×10^{-28}
Socs1	2.47	2.93×10^{-09}	3.37	9.18×10^{-13}
Tgtp1	4.27	1.11×10^{-17}	6.68	6.95×10^{-25}
Tgtp2	2.58	1.04×10^{-16}	5.37	1.79×10^{-28}
$CD8^+$ Naive T cells				
Bcl3	3.12	7.66×10^{-15}	3.33	5.29×10^{-15}
Csf1	2.42	3.64×10^{-6}	4.35	1.61×10^{-11}
F2rl2	2.03	5.14×10^{-4}	3.22	2.22×10^{-6}
Gadd45g	5.15	1.07×10^{-13}	2.74	1.27×10^{-5}
Gata1	3.12	5.10×10^{-9}	4.38	2.86×10^{-12}
Gbp10	3.19	1.04×10^{-7}	6.16	5.29×10^{-15}
Gbp11_1	5.25	9.02×10^{-18}	4.71	1.63×10^{-15}
Gbp6_1	2.88	3.60×10^{-6}	5.24	1.10×10^{-11}
Gem	2.49	3.02×10^{-6}	2.60	1.36×10^{-5}
Gm12185	2.45	1.66×10^{-15}	3.68	4.72×10^{-21}
Gzmb	3.01	4.27×10^{-6}	2.54	7.63×10^{-4}
Ifi47	3.61	3.08×10^{-12}	4.22	1.62×10^{-13}
Igtp	3.48	6.54×10^{-21}	5.14	8.05×10^{-27}
Iigp1	2.62	1.44×10^{-10}	6.19	3.57×10^{-22}
Il12rb2	3.37	1.06×10^{-4}	4.22	2.47×10^{-5}
Jun	3.65	2.39×10^{-18}	3.47	6.86×10^{-17}
Pim2	3.38	1.20×10^{-31}	2.99	1.56×10^{-28}
Serpina3g	3.40	1.43×10^{-6}	4.75	5.86×10^{-9}
Tgtp1	3.77	2.66×10^{-16}	5.38	3.50×10^{-21}
Tgtp2	2.59	3.55×10^{-17}	4.59	1.05×10^{-25}

Lists of DEGs; their log_2 (fold changes [FC]) and adjusted *P* values generated for each condition were compared using Venn diagrams to obtain the list of overlapping genes between IL-7 and IFN-γ stimulation in WT T cells. [A]FC were calculated relative to unstimulated condition for each sample.

higher expression of STAT1 than the WT cells (Figure 5B). Smaller expression changes were noted in FP donor T cells from both strains (Figure 5B). No changes were observed in IL-7Rα expression, except for the slow proliferating STAT1 Tg $CD4^+$ T cells (Supplemental Figure 5A). In addition, increased p-STAT1 upon in vitro stimulation with IL-7 was observed in SP cells compared with the baseline before adoptive transfer (Figure 5C), and no changes were observed in activation of STAT5 (Supplemental Figure 5B). Despite higher expression of STAT1 in SP STAT1 Tg donor T cells compared with WT donor T cells, no differences were observed in p-STAT1 levels upon in vitro stimulation with IFN-γ (Supplemental Figure 5C).

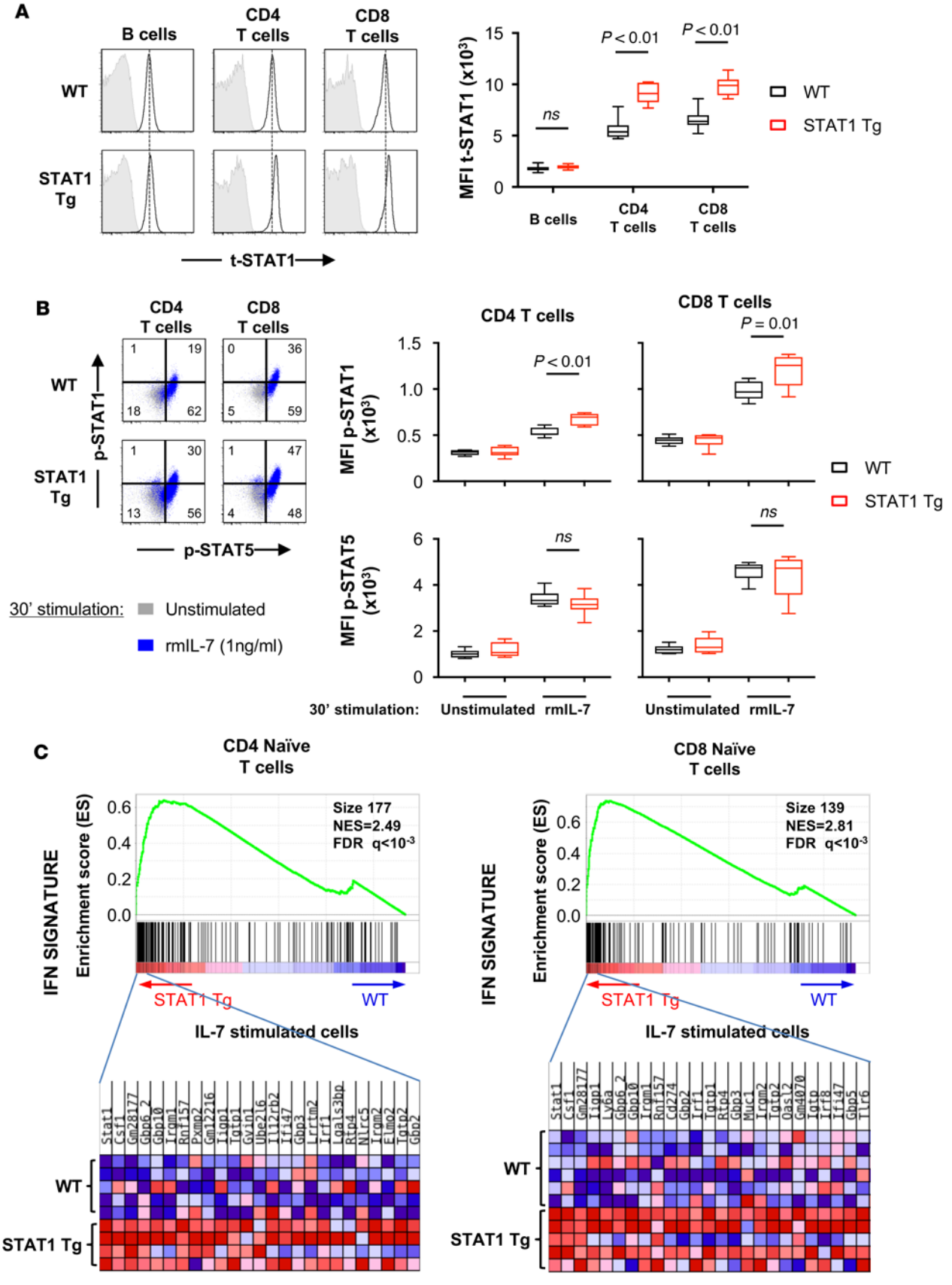
A
B cells
CD4 T cells
CD8 T cells
WT
STAT1 Tg
t-STAT1
MFI t-STAT1 (x10³)
P < 0.01
P < 0.01
ns
WT
STAT1 Tg
B
p-STAT1
p-STAT5
CD4 T cells
CD8 T cells
MFI p-STAT1 (x10³)
MFI p-STAT5 (x10³)
P = 0.01
30' stimulation:
Unstimulated
rmIL-7 (1ng/ml)
C
CD4 Naïve T cells
CD8 Naïve T cells
IFN SIGNATURE
Enrichment score (ES)
Size 177
NES=2.49
FDR q<10⁻³
Size 139
NES=2.81
FDR q<10⁻³
STAT1 Tg
WT
IL-7 stimulated cells

Figure 4. STAT1 overexpression in T cells leads to activation of STAT1 and STAT5 in response to IL-7. LN cells from WT (n = 10) and STAT1 Tg (n = 10) mice were analyzed by flow cytometry for expression of (**A**) t-STAT1 and (**B**) phosphorylated STAT1 and STAT5 after in vitro stimulation with rmIL-7 (1 ng/ml) in B cells ($CD3^-$ $B220^+$), $CD4^+$ ($B220^-$ $CD3^+$ $CD4^+$), and $CD8^+$ ($B220^-$ $CD3^+$ $CD8^+$) T cells. Shaded histograms represent isotype control staining. The MFIs of t-STAT1, p-STAT1, and p-STAT5 in the different populations were compared between WT (black symbols) and STAT1 Tg (red symbols) mice using a nonparametric Mann-Whitney test. Data from 3 independent experiments, including an average of 3–4 mice per group per experiment, are presented as box and whisker plots showing the median MFI value bounded by the first and third quartiles in the box, with whiskers extending to the minimum and maximum values. (**C**) Gene set enrichment analysis (GSEA) histograms of IFN signature in STAT1 Tg versus WT $CD4^+$ and $CD8^+$ naive T cells stimulated with IL-7. The enrichment score (ES; y axis) reflects the degree to which IFN signature was enriched in STAT1 Tg vs. WT T cells. Each solid bar represents 1 gene within IFN signature. The heat-map image illustrates the gene expression levels of the leading edge subset. The normalized enrichment score (NES) and false discovery rate (FDR) q value are indicated.

The examination of the donor T cell counts in the LNs showed approximately half reduction of $CD4^+$ T cell numbers of recipients transferred with STAT1 Tg T cells compared with WT cells (Figure 6A). A similar trend was observed for $CD8^+$ donor T cell numbers from STAT1 Tg mice (Figure 6A). Additionally, the decreased STAT1 Tg $CD4^+$ T cell donor numbers in the LNs were more pronounced for naive and the effector/effector memory and CD8 naive phenotypes (Figure 6B). The reduction in the number of $CD4^+$ T cells in LNs was not accounted for by accumulation of donor cells in the spleens of the STAT1 Tg mice (data not shown). In addition, WT and STAT1 Tg T cells undergoing LIP showed similar acquisition of memory-like phenotype and showed similar levels of IFN-γ secretion after in vitro stimulation with PMA/ionomycin, suggesting a similar activation of these cells (Figure 6C). Thus, these data suggest that overexpression of t-STAT1 in T cells undergoing IL-7–dependent LIP led to impaired $CD4^+$ T cell homeostatic reconstitution.

Discussion

In the present manuscript, we describe that, in steady-state conditions, IL-7 signaling regulates a set of STAT1/IFN-associated mRNA transcripts, which are enriched in conditions of increased STAT1 expression, such as lymphopenia. In addition, overexpression of STAT1 limits $CD4^+$ T cell reconstitution. Our data suggest a model in which T cells undergoing LIP upregulate expression of STAT1, "switching on" an IL-7–dependent STAT1/STAT5 activation that could regulate $CD4^+$ T cell expansion. This mechanism could be a physiological mechanism to regulate the expansion and the size of the $CD4^+$ T cell pool under lymphopenic conditions.

It has been described that IL-7/IL-7R signaling can activate — in addition to STAT5 — STAT1 and STAT3, but the function of IL-7-dependent activation of these transcription factors are largely unknown (34–36). In the present manuscript, we present evidence of the contribution of IL-7–dependent STAT1 activation limiting the expansion of the $CD4^+$ T cell pool. T cell homeostasis is a mechanism designed to maintain a relatively constant size and repertoire of the T cell pools throughout life. This is achieved by slow proliferation of T cells in the periphery mediated by IL-7 (11). In contrast, in lymphopenic hosts, adoptively transferred T cells undergo a robust proliferation in which $CD4^+$ T cells show a slower proliferation than that observed in $CD8^+$ T cells (11). Similarly, under clinic settings of lymphopenia, such as extensive chemotherapy and BM transplant, $CD4^+$ T cell reconstitution is slow and can take more than a year to achieve full reconstitution. Distinct reconstitution is observed in the $CD8^+$ T cell pool in which cells undergo a profound proliferation accompanied by accumulation of cells with an activated memory-like phenotype (13–15, 17, 40). This reconstitution profile is also observed in patients with HIV infection in whom complete $CD4^+$ T cell reconstitution following cART therapy is a slow process that typically requires many years and depends on the $CD4^+$ T cell number prior to therapy and other factors (17–19). In the HIV infection, $CD8^+$ T cell numbers are already expanded, and the $CD8^+$ T cell pool does not seem to be influenced by the degree of $CD4^+$ T cell depletion. Moreover, while the $CD8^+$ T cell pool shows great expansion potential, the $CD4^+$ T cell pool seems to be highly regulated in their capacity for expansion (16, 24). Previously, we had shown that, in HIV-infected patients, the immune activation of naive $CD4^+$ T cells (measured as proliferation) is mainly driven by $CD4^+$ T cell depletion. In contrast, the immune activation of the memory $CD4^+$ T cells is driven by a combination of homeostatic forces (CD4 counts) and viral replication, and both subsets showed increased mRNA expression of transcripts associated with γc cytokines and type I IFNs (24). HIV-infected patients showed increased expression of t-STAT1, suggesting that IL-7 signaling in $CD4^+$ T cells undergoing homeostatic proliferation may be driven by activation of STAT1 and STAT5. These pathways could contribute to the slow recovery of the $CD4^+$ T cell pool following cART (37,

Table 3. Top 15 most-affected categories of diseases and biological functions predicted by IPA within DEGs in WT and STAT1 Tg CD4⁺ naive T cells stimulated 90 minutes with IL-7

	WT cells stimulated with IL-7				STAT1 Tg cells stimulated with IL-7				
Diseases or functions annotation	***P* value[A]**	**Predicted activation state**	**Activation Z score[B]**	**# Mol[C]**	**Diseases or functions annotation**	***P* value**	**Predicted activation state**	**Activation Z score**	**# Mol**
90' stimulation									
Generation of cells	1.26×10^{-12}	Increased	3.47	134	**Generation of cells**	1.77×10^{-12}	Increased	3.18	133
Proliferation of cells	3.16×10^{-16}	Increased	3.22	221	**Morbidity or mortality**	2.57×10^{-08}	Decreased	−3.14	137
Development of blood cells	6.08×10^{-20}	Increased	3.12	79	**Organismal death**	1.15×10^{-7}	Decreased	−3.01	133
Proliferation of epithelial cells	3.22×10^{-10}	Increased	3.05	46	**Bacterial Infections**	4.81×10^{-10}	Decreased	−2.86	40
Cell survival	5.35×10^{-10}	Increased	3.02	95	**Formation of osteoclasts**	2.14×10^{-6}	Increased	2.71	15
Development of leukocytes	3.85×10^{-22}	Increased	2.99	77	**Cell viability of mononuclear leukocytes**	6.46×10^{-12}	Increased	2.66	28
Proliferation of blood cells	1.15×10^{-20}	Increased	2.95	89	**Development of blood cells**	2.24×10^{-18}	Increased	2.64	76
Morbidity or mortality	2.47×10^{-10}	Decreased	−2.94	145	**Transactivation of RNA**	8.51×10^{-9}	Increased	2.60	46
Activation of T lymphocytes	1.08×10^{-10}	Increased	2.91	38	**Cell survival**	1.86×10^{-9}	Increased	2.54	93
Organismal death	4.57×10^{-9}	Decreased	−2.88	139	**Development of leukocytes**	4.83×10^{-21}	Increased	2.52	75
Transactivation of RNA	1.20×10^{-9}	Increased	2.76	48	**Cell viability of lymphocytes**	1.12×10^{-11}	Increased	2.50	27
Proliferation of lymphocytes	4.87×10^{-21}	Increased	2.72	82	**Activation of cells**	1.83×10^{-15}	Increased	2.43	86
Development of lymphocytes	1.02×10^{-22}	Increased	2.70	74	**Lymphatic node tumor**	1.96×10^{-8}	Increased	2.42	48
Malignant solid tumor	5.68×10^{-14}	Increased	2.62	488	**Infection of mammalia**	4.63×10^{-14}	Decreased	−2.39	42
Proliferation of mononuclear leukocytes	3.06×10^{-21}	Increased	2.62	83	**Activation of mononuclear leukocytes**	1.58×10^{-14}	Increased	2.38	53

Lists of DEGs; their $\log_2$ (FC) and adjusted *p* values were generated for WT and STAT1 Tg CD4⁺ T cells stimulated for 90 minutes with rmIL-7 and used as input in IPA software. [A]The *P* value was calculated with the Fischer's exact test and reflects the likelyhood that the association between a set of genes in dataset and a related biological function is significant. [B]A positive or negative Z score value indicates that a function is predicted to be increased or decreased in T cells stimulated with IL-7. [C]Number of RNAs differentially expressed in the disease and functions category.

24). The direct cytopathic effect of HIV plays an important role, although it does not completely explain the depletion of the CD4⁺ T cell pool. We have shown that, in the context of lymphopenia, IL-7 drives increased expression of STAT1, enhancing the response to type I IFNs. In addition, in the setting of chronic exposure to type I IFNs, this mechanism led to the preferential depletion of the CD4 effector memory phenotype (37). The present data suggest that HIV alters T cell homeostasis and cytokine responses, leading to the depletion of the CD4⁺ T cell pool.

Together, these observations suggest that factors directly and indirectly associated with the virus contribute to the activation and depletion of the CD4⁺ T cell pool in these patients. More studies should be directed to address the mechanism of IL-7–dependent upregulation of STAT1. Blockade of STAT1 upregulation may promote greater and faster reconstitution of the CD4⁺ T cell pool following cART. In addition, it has been shown that homeostatic proliferation participates in the establishment and maintenance of cells harboring HIV provirus (41, 42). Therefore, it would be important to consider the potential impact of blocking STAT1-dependent IL-7 signaling on the viral reservoir. The present data suggest a potential mechanism to the observations that suggest that the CD4⁺ and CD8⁺ T cell pools may respond differentially to a lymphopenic environment, and/or they possess a distinct homeostatic regulatory mechanism that may explain these differences. While the CD4⁺ T cell pool is highly regulated in size, CD8⁺ T cells can undergo greater expansions.

Table 4. Top 15 most-affected categories of diseases and biological functions predicted by IPA within DEGs in WT and STAT1 Tg CD4⁺ naive T cells stimulated overnight with IL-7

	WT cells stimulated with IL-7				STAT1 Tg cells stimulated with IL-7				
Diseases or functions annotation	***P* value[A]**	**Predicted activation state**	**Activation Z score[B]**	**# Mol[C]**	**Diseases or functions annotation**	***P* value**	**Predicted activation state**	**Activation Z score**	**# Mol**
Overnight stimulation									
Organismal death	1.30×10^{-14}	Increased	8.24	495	**Organismal death**	4.70×10^{-16}	Increased	9.28	550
Morbidity or mortality	1.17×10^{-14}	Increased	7.76	501	**Morbidity or mortality**	5.64×10^{-16}	Increased	8.77	556
Cell survival	2.27×10^{-16}	Decreased	−4.88	321	**Cell survival**	3.54×10^{-18}	Decreased	−6.27	357
Cell viability	1.69×10^{-14}	Decreased	−4.43	296	**Cell viability**	5.00×10^{-16}	Decreased	−5.61	329
Cellular homeostasis	6.62×10^{-17}	Decreased	−3.94	352	**Cell movement**	4.24×10^{-17}	Decreased	−4.25	505
Proliferation of cells	6.90×10^{-33}	Decreased	−3.44	809	**Cell viability of tumor cell lines**	4.68×10^{-12}	Decreased	−4.01	202
Antibody response	3.66×10^{-7}	Decreased	−3.20	44	**Survival of organism**	1.12×10^{-11}	Decreased	−3.96	183
Survival of organism	$8.98 \times 1^{0-12}$	Decreased	−3.16	169	**Migration of cells**	9.15×10^{-17}	Decreased	−3.89	458
Cell viability of blood cells	7.94×10^{-9}	Decreased	−3.15	74	**Cellular homeostasis**	2.09×10^{-15}	Decreased	−3.80	377
Cell movement	7.97×10^{-15}	Decreased	−3.06	451	**Proliferation of cells**	1.92×10^{-34}	Decreased	−3.75	891
Inflammation of body cavity	4.66×10^{-8}	Increased	3.03	169	**Cell viability of blood cells**	5.09×10^{-10}	Decreased	−3.56	83
Immune response of leukocytes	4.66×10^{-7}	Decreased	−3.00	73	**Generation of cells**	1.38×10^{-19}	Decreased	−3.54	495
Cell viability of leukocytes	1.22×10^{-9}	Decreased	−2.95	70	**Outgrowth of cells**	5.78×10^{-7}	Decreased	−3.35	106
Synthesis of lipid	2.45×10^{-6}	Decreased	−2.83	148	**Invasion of cells**	6.03×10^{-7}	Decreased	−3.27	198
Cell viability of tumor cell lines	9.45×10^{-10}	Decreased	−2.83	177	**Development of blood cells**	7.28×10^{-23}	Decreased	−3.23	223

Lists of DEGs; their $\log_2$ (FC) and adjusted *p* values were generated for WT and STAT1 Tg CD4⁺ T cells stimulated for overnight with rmIL-7 and used as input in IPA software. [A]The *P* value was calculated with the Fischer's exact test and reflects the likelyhood that the association between a set of genes in dataset and a related biological function is significant. [B]A positive or negative Z score value indicates that a function is predicted to be increased or decreased in T cells stimulated with IL-7. [C]Number of RNAs differentially expressed in the disease and functions category.

We found that, under steady-state conditions, in vitro stimulation with IL-7 can induce mRNA transcripts associated to STAT1/IFN in naive WT T cells, and these genes were enriched in T cells overexpressing STAT1. We showed that, while IL-7 promotes proliferation and survival of T cells, it also showed proapoptotic potential (Supplemental Figure 4D, Table 3, Table 4, Supplemental Table 6, and Supplemental Table 8). Recent reports had shown that IL-7 in vitro and in vivo in T cells undergoing homeostatic proliferation induces secretion of IFN-γ (43). Continuous IL-7 signaling leads to an IFN-γ–dependent induced cell death in CD8⁺ T cells (44). This pathway may contribute to the homeostasis of the CD4⁺ T cell pool by increasing STAT1 expression and generating a positive loop of transcription of STAT1 and its associated genes. However, overexpression of STAT1 on T cells undergoing LIP did not lead to increased secretion of IFN-γ, nor to an enhanced responsiveness to in vitro stimulation with IFN-γ. Moreover, recent reports had shown that STAT1 can affect survival and proliferation in T cells, and this effect is partially independent of IFN-γ signaling (45). These data and our observations suggest that STAT1 may be involved in balancing proliferation and anti- and pro-apoptotic signals during lymphopenia. In addition, IL-7 signaling activates the PI3K/AKT pathway, which constitutes a critical signal for survival and proliferation (11). Cytokines such as type I IFNs can regulate the AKT pathway in T cells and mediate antiproliferative effects. Whether IL-7–dependent STAT1 activation regulates AKT pathway needs further investigation (46). Our model suggests that CD4⁺ T cell expansion in cells undergoing LIP is regulated by an IL-7–dependent signaling composed by activation of STAT1 and STAT5, and this mechanism limits the expansion of the CD4⁺ T cell pool.

The transcription of STAT1/IFN-associated genes may also reflect other potential properties of IL-7 (47, 48). Recently, we have described that IL-7 can potentiate the responsiveness of T cells to type I IFNs by modulating the expression levels of STAT1 (37). In the present study, we found that IL-7 induces in STAT1 Tg T cells mRNA transcripts of IFN-inducible GTPases, such as those that belong to the GBP

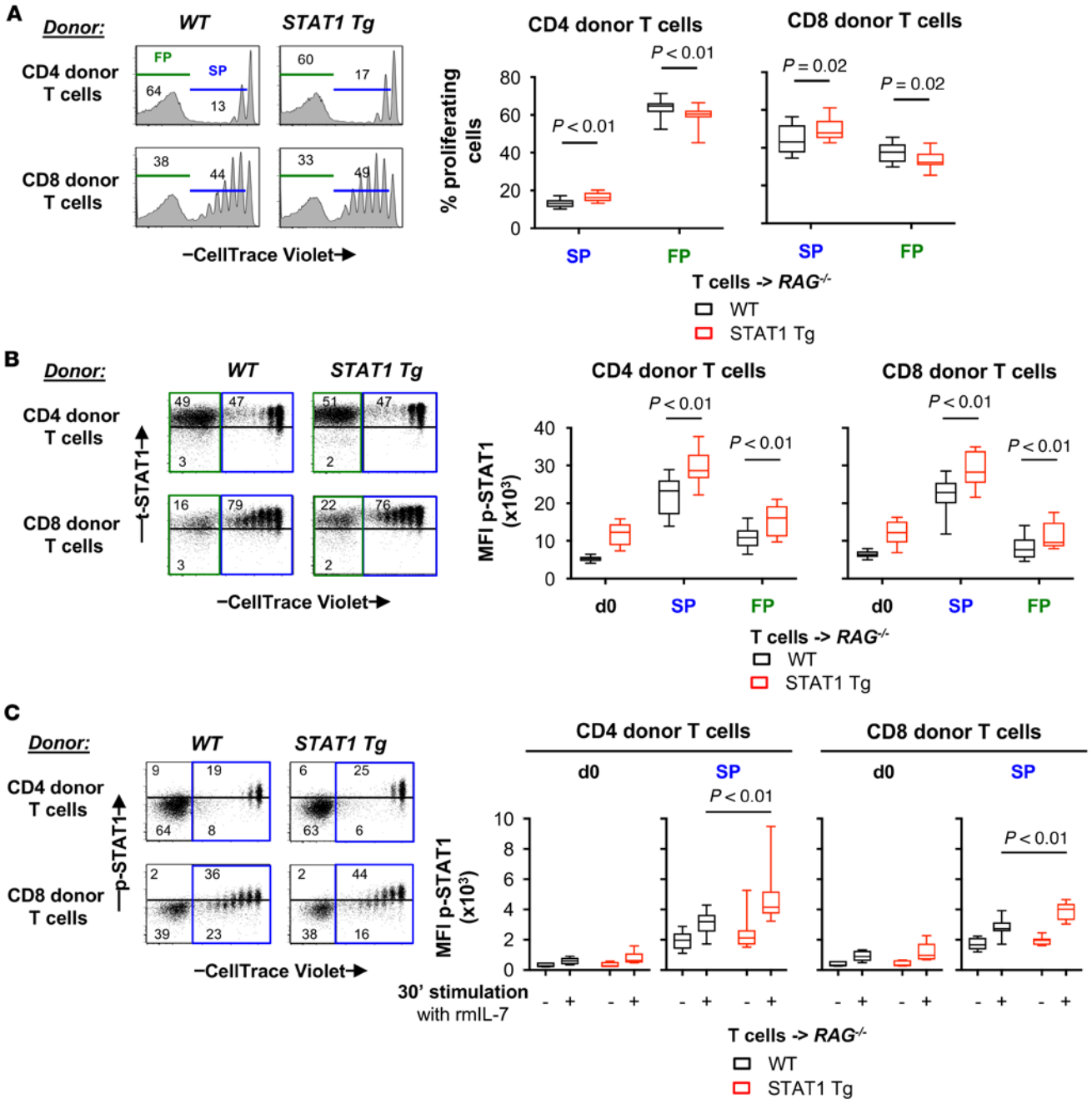

Figure 5. Adoptive transfer of STAT1 Tg T cells into lymphopenic RAG$^{-/-}$ mice leads to increase STAT1 expression in proliferating T cells. Lymphopenic *RAG*$^{-/-}$ mice were injected i.v. with 6 × 10^6 of CTV-labeled T cells isolated from the LNs of congenic WT or STAT1 Tg mice. Analysis of donor cells in LNs was performed on day 7 after transfer. (**A**) Percentages of slow and fast proliferating (SP, CTV$^+$ cells gated in blue; FP, CTV$^-$ cells gated in green) CD45.2$^+$ CD3$^+$ CD4$^+$ and CD8$^+$ donor lymphocytes are shown. (**B**) The percentages of donor T cells CTV$^+$ t-STAT1^{high}, CTV$^-$ t-STAT1^{high}, and CTV$^-$ t-STAT1^{low} are indicated. The MFIs of t-STAT1 in CD4$^+$ and CD8$^+$ donor T cells before (d0) and after adoptive transfer (SP and FP) with WT (n = 13, black symbols) or STAT1 Tg (n = 15, red symbols) were compared using a nonparametric Mann-Whitney test. (**C**) The percentages of donor T cells CTV$^+$ p-STAT1^{high}, CTV$^+$ p-STAT1^{low}, CTV$^-$ p-STAT1^{high}, and CTV$^-$ p-STAT1^{low} are indicated. The MFIs of p-STAT1 in CD4$^+$ and CD8$^+$ donor T cells before (d0) and after adoptive transfer into *RAG*$^{-/-}$ mice (SP) were compared as described above. Data are from 4 independent experiments out of 4, including an average of 3–4 mice per group per experiment and presented as box and whisker plots showing the median value bounded by the first and third quartiles in the box, with whiskers extending to the minimum and maximum values.

and IRG protein families. Particularly, the members of the IRG family have been involved in immunity against pathogens; however, emerging data suggest that they may also play a role in T cell homeostasis (49). Together, these observations suggest that IL-7 may play a role in immunity against pathogens modulating its own signaling and that of other cytokines.

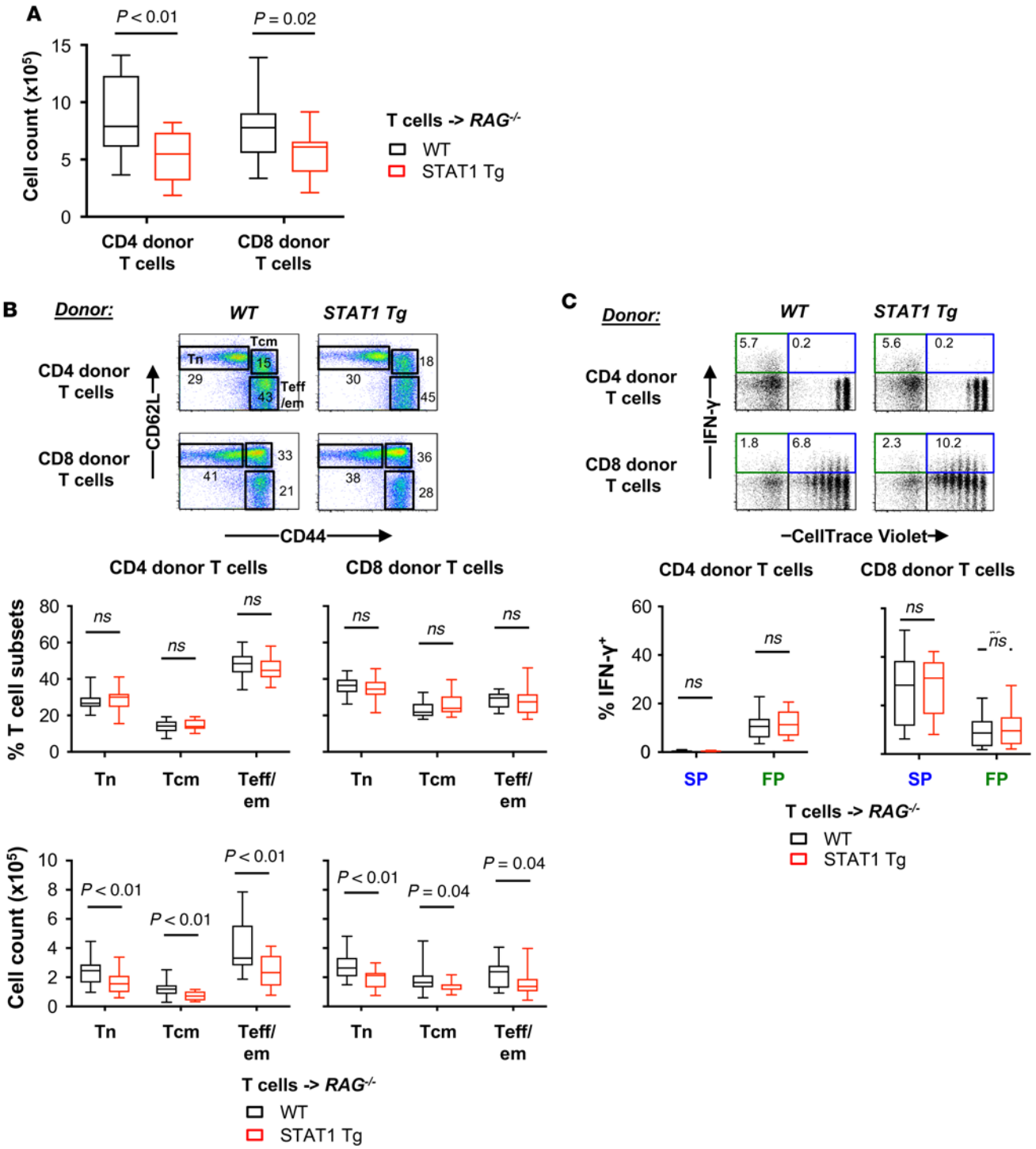

Figure 6. Adoptive transfer of STAT1 Tg T cells into lymphopenic *RAG*$^{-/-}$ mice leads to long-term impaired CD4$^+$ T cell reconstitution. Lymphopenic *RAG*$^{-/-}$ mice transferred with WT (n = 16) or STAT1 Tg (n = 15) T cells were analyzed as described above. (**A**) Absolute numbers of CD4$^+$ and CD8$^+$ donor T cells were enumerated following T cell transfer with WT (black symbols) or STAT1 Tg (red symbols) cells. (**B**) Expression of CD44 and CD62L on CD4$^+$ and CD8$^+$ donor T cells was assessed by flow cytometry in LNs. The percentages and absolute cell counts of CD4$^+$ and CD8$^+$ donor T cell subsets in *RAG*$^{-/-}$ mice transferred with WT (black symbols) or STAT1 Tg (red symbols) T cells are presented. (**C**) LN cells were stimulated ex vivo with PMA/ionomycin. IFN-γ production by donor T cells was assessed by intracellular staining, and plots represent CFSE fluorescence versus IFN-γ on gated CD45.2$^+$ CD3$^+$ CD4$^+$ and CD8$^+$ lymphocytes. The percentages of IFN-γ–producing donor T cells are indicated. Background in nonstimulated controls was < 1%. A nonparametric Mann-Whitney test was performed for comparisons between groups. Data are from 5 independent experiments out of 5, including an average of 3–4 mice per group per experiment and presented as box and whisker plots showing the median value bounded by the first and third quartiles in the box, with whiskers extending to the minimum and maximum values.

In the present manuscript, we describe a pathway in which IL-7 can modulate its own signaling. IL-7 can regulate the expression levels of STAT1, "turning on" an IL-7–dependent STAT1 activation in addition to STAT5, controlling the expansion of the $CD4^+$ T cell pool under lymphopenic conditions. In chronic HIV infection, the mechanisms behind the steady decline of the $CD4^+$ T cells are not very well understood, and the direct cytopathic effect of the virus does not explain this outcome. HIV may take advantage of this physiological pathway, causing the immune dysregulation of the $CD4^+$ and $CD8^+$ T cell pools observed in these patients. Therapeutic strategies targeting this pathway may enhance T cell reconstitution in the clinical settings of lymphopenia.

Methods

Patient and healthy volunteers. Healthy volunteers were obtained through the NIH blood bank. The majority of the patients studied had chronic HIV infection. The cohort of HIV-infected patients used to assess the relationship between STAT1 phosphorylation after in vitro stimulation with IL-7 and t-STAT1 levels consisted of patients (n = 53) who had successfully suppressed viremia (viral load < 50 copies/ml) with cART for more than 9 months. The patients and healthy control characteristics are described in Table 1.

Mice. B6.SJL-[KO]RAG1 ($RAG^{-/-}$) mice were purchased from Taconic and then housed at the NIAID, Building 50 Shared Animal Facility (50SAF). STAT1 Tg mice and WT littermates were generated and maintained under specific pathogen-free conditions in the NIAID 50SAF. The STAT1 Tg construct was generated by ligating a murine STAT1 cDNA into human CD2 (hCD2) enhancer-promoter–based vectors and injected into fertilized B6 oocytes to generate STAT1 Tg mice. Three founder mice were born and crossed to generated F1 progeny with integration of the transgene. The following experiments were performed with mice derived from the founder animal expressing the higher level of the transgene. All mice used in these studies were between 5 and 13 weeks of age.

A mixture of inguinal, axillary, cervical, mandibular, popliteal, and mesenteric LNs were excised from WT or STAT1 Tg mice and processed to obtain single cell suspensions by mechanic disruption on Nitex filters in RPMI 1640 medium (Cellgro) containing 10% FCS, 55 μM β-mercaptoethanol, 2 mM L-glutamine, and 50 μg/ml gentamicin (Cellgro, Corning) at 4°C. After counting, cells from LNs were stained with the indicated Abs and/or stimulated in vitro with IL-7 (see blow).

Cell culture and Western blot. PBMCs from healthy controls were obtained by Ficoll gradient centrifugation. $CD4^+$ T cells were isolated by negative selection (Miltenyi Biotec) and cultured in X-VIVO 15 medium (Lonza) in the absence or presence of rhIL-7 (10 ng/ml; Peprotech). After 3 days of culture, the cells were harvested, washed with cytokine-free medium, and adjusted at a concentration of 2×10^6 cells/ml prior to resting overnight for subsequent in vitro stimulation for 30 minutes at 37°C and 5% CO_2 stimulation with previously defined optimal dose of rhIL-7 (1 ng/ml). The stimulation was terminated by adding an equal volume of cold-temperature PBS containing phosphatase inhibitor to prevent dephosphorylation of the activated STATs (Thermo Fisher Scientific). After 3 washes with cold-temperature PBS containing phosphatase inhibitor, the samples were stored at –20°C as dry pellets. Whole cell lysates were prepared from these samples with RIPA lysis buffer containing 50 mM Tris-HCl pH 7.5, 150 mM NaCl, 1% Nonidet P-40, 0.1% SDS, 0.5% sodium deoxycholate supplemented with protease inhibitor and phosphatase inhibitor cocktails (Pierce, Thermo Scientific) before use. Antibodies to STAT1 (catalog sc-346) and STAT5 (catalog sc-835) were from Santa Cruz Biotechnology Inc. Phosphorylation-specific antibodies to STAT1 (Tyr701; catalog 9171) and STAT5 (Tyr694; catalog 9351) were from Cell Signaling Technology. After detection of the target protein, the membrane was stripped and reprobed with anti–β-actin antibody (clone mAbcam 8226; Abcam, ab8226) to assess loading equivalency.

Preparation of CTV-labeled cells and adoptive transfer. T cells from STAT1 Tg and WT littermate mice were prepared from single cell LN suspensions by magnetic depletion using the T cell isolation kit and LS columns from Miltenyi Biotec according to the manufacturer's instructions. T cell purity was greater than 90%. Purified T cells were labeled with 5 μM CTV (Invitrogen) in PBS as described above. CTV-labeled T cells (6×10^6)from STAT1 Tg or WT littermate mice were transferred by i.v. injection into lymphopenic $RAG^{-/-}$ recipient mice.

Seven days after transfer, a mixture of inguinal, axillary, cervical, mandibular, popliteal, and mesenteric LN were excised, processed, and analyzed as described above.

In vitro stimulation with IL-7. For the human study, frozen PBMCs from patients and healthy controls were thawed and rested overnight before stimulation and staining. The next day, cells were washed and labeled with live/dead (Invitrogen). Adjusted at a concentration of 2×10^6 cells/ml, cells were then incubated for 30 minutes at 37°C and 5% CO_2 with 1 ng/ml rhIL-7, and p-STAT1 levels were analyzed by flow cytometry.

For mouse experiments, LN cells were adjusted at a concentration of 2×10^6 cells/ml and rested for at least 1 hour in a cytokine-free complete medium. Cells were then incubated for 30 minutes at 37°C and 5% CO_2 with 1 ng/ml recombinant murine IL-17 (rmIL-7, Peprotech), and p-STAT1 and p-STAT5 levels were analyzed by flow cytometry.

Flow cytometry. IL-7 stimulations were stopped by fixation with 4% paraformaldehyde, followed by a permeabilization step with 1:1 methanol/acetone mix for 30 minutes on ice.

For human PBMCs, after 3 washes, cells were incubated for 10 minutes with 10 μg/ml human IgG (MilliporeSigma) to block potential Fc receptor binding and stained for 1 hour at room temperature with anti–CD3 Qdot 605 (clone UCHT1; Invitrogen, Q10054), anti–CD4 Pacific blue (clone RPA-T4; BD Biosciences, 558116), anti–STAT1 N-terminus Alexa Fluor 647 (clone 1/Stat1; BD Biosciences, 558560), and anti–tyrosine 701-phosphorylated STAT1 Alexa Fluor 488 (clone 58D6; Cell Signaling Technology, 9174).

For murine experiments, after 3 washes, mouse lymphocytes were stained for 30 minutes at room temperature with a mix of anti–tyrosine 701 phosphorylated STAT1 Alexa Fluor 488 and anti–STAT1 N-terminus Alexa Fluor 647 or anti–tyrosine 694-phosphorylated STAT5 Alexa Fluor 647 (clone 47; BD Biosciences, 612599), followed by an additional 20 minutes incubation at room temperature with a mix of anti–CD3 PE-Cy7 (clone 17A2; BD Biosciences, 560591), anti–CD4 PerCP-Cy5.5 (clone RM4-5; eBioscience, 45-0042), anti–CD8α eFluor 650NC (clone 53-6.7; eBioscience, 86-0081), anti–B220-PE (clone RA3-6B2; BioLegend, 103208), and anti-CD16/CD32 (clone 2.4G2; BD Biosciences, 553141). Fluorescence-minus-1 controls were performed in the Alexa Fluor 647 and Alexa Fluor 488 channel for control of compensation spread (50).

Phenotype and intensity of CTV fluorescence were analyzed in fresh, unstimulated mouse lymphocytes. Donor T cells were detected by virtue of their CD45.2 expression. Antibodies purchased from eBioscience with the following specificities were used for staining: anti–CD45.2 PE (clone 104; 12-0454), anti–CD3 PE-Cy7, anti–CD4 PerCP-Cy5.5, anti–CD8α eFluor 650NC, anti–CD44 APC-eFluor 780 (clone IM7; 47-0441), anti–CD62L eFluor 605 (clone MEL-14; 93-0621), and anti–CD127 APC (IL-7Rα; clone A7R34; 17-1271).

To assess production of IFN-γ by $CD4^+$ and $CD8^+$ donor T cells after adoptive transfer, LN cells were incubated in complete media with 10 ng/ml PMA (MilliporeSigma), 1 μM ionomycin (MilliporeSigma), and10 μg/ml brefeldin A (Calbiochem) for 4 hours at 37°C. Cells that were not stimulated with PMA/ionomycin were used as a negative control. After washing, cells were stained to detect cell-surface CD45.2, CD3, CD4, and CD8 as described above. Cells were then permeabilized and stained to detect intracellular IFN-γ with an anti–IFN-γ-APC mAb (clone XMG1.2; BD Biosciences, 554413) using the Cytofix/Cytoperm kit (BD Biosciences) according to the manufacturer's instruction.

Human samples were collected on a BD LSR II, and mouse samples were collected on a BD LSR Fortessa using FACSDiva software. Data were subsequently analyzed using FlowJo (Tree Star Inc.).

mRNA-Seq and transcriptome analysis. $CD4^+$ and $CD8^+$ naive T cells from LNs of STAT1 Tg (n = 4 and 5, respectively) and WT littermate (n = 5 and 6, respectively) mice were sorted on a BD FACS Aria based on surface staining of $CD8^-$ $CD4^+$ $CD44^{low}$ $CD62L^+$ and $CD8^+$ $CD4^-$ $CD44^{low}$ $CD62L^+$ cell populations respectively. A mix of anti-B220, anti-CD49d (clone DX5; BioLegend, 108908), anti-Ter119 (clone TER-119; BioLegend, 116208), anti–MHC-II (clone M5/114.15.2; eBioscience, 12-5321), and anti–Gr-1 (clone RB6-8C5; BioLegend, 108408) was used in PE as a dump channel. Sorted cell populations were spun down and adjusted at a concentration of 2×10^6 cells/ml prior to resting overnight for subsequent in vitro stimulation for 90 minutes at 37°C and 5% CO_2 in presence or not of rmIL-7 (10 ng/ml) or rmIFN-γ (10 ng/ml; Peprotech). The samples were then washed once with PBS before being resuspended in TRIzol (Invitrogen) and stored at –80°C.

Stranded mRNA-Seq libraries were generated using Illumina TrueSeq Stranded mRNA Library Prep kit from an input of 500 ng total RNA. Libraries were sequenced to read lengths of at least 75 bp, paired-end strategy, as multiplexed pools on an Illumina NextSeq500 (v2 chemstry) to a read depth of approximately 30 million fragments per library. Trimmed reads were aligned to mouse genome version GRCm38 and mapped to ensemble gene features (v38.80, current June 2015) using Genomics Workbench software (CLC bio, version 8.0.2). Complete read-pairs mapping to specific (10 or fewer) exon locations were counted. Reads matching (10 or fewer) equally high-scoring locations were assigned randomly. Using JMP/Genomics software (SAS Institute), raw counts were inflated, log-transformed, and then normalized by upper quartile scaling, followed by ANOVA test for differential gene expression. Differential expression P values were adjusted for multiple testing using the false discovery rate method of Benjamini-Hochberg.

DEGs were selected with the following criteria: (i) adjusted $P < 0.05$ and (ii) fold change (FC) relative to unstimulated condition ≥ I2I (FC ≥ 2 or ≤ –2). Tables including the list of DEGs, their $\log_2$ (FC), and adjusted P values were generated for each condition. An IFN signature was defined based on the list of DEGs in WT T cells stimulated in vitro with IFN-γ.

Venn diagrams were drawn using Bioinformatics & Evolutionary Genomics web tools (http://bioinformatics.psb.ugent.be/webtools/Venn/). IPA (QIAGEN) software was used for upstream regulator and categories of diseases and biological functions analyses within DEGs identified in this study. GSEA was performed to determine whether the IFN signature is enriched within WT and STAT1 Tg T cell samples stimulated in vitro with IL-7. GSEA was performed to analyze the enrichment of the gene set following the developer's protocol (51) (http://www.broad.mit.edu/gsea/). All original microarray data were deposited in the NCBI's Gene Expression Omnibus database (GEO GSE106575).

Statistics. For the human study, Spearman's rank correlation coefficients were used to assess the association of t-STAT1 expression and STAT1 phosphorylation after in vitro IL-7 stimulation in Figure 1. Nonparametric unpaired Mann-Whitney tests were used to analyze the data from the mouse experiments. Data were considered to be statistically different if $P < 0.05$.

Study approval. The human study was conducted according to the principles expressed in the Declaration of Helsinki. Patients were studied under a NIAID IRB–approved HIV clinical research study protocol in the NIAID/CCMD intramural program. Patients and healthy controls provided written informed consent for the collection of samples and subsequent analysis. Healthy volunteers were obtained through the NIH blood bank.

All animal work was conducted according to relevant national and international guidelines. The animal experiments were performed under a study protocol approved by the NIAID Animal Care and Use Committee (Animal Study Proposal protocol LIR2E).

Author contributions

CLS performed the experiments, analyzed and interpreted data, and wrote the manuscript. MAL and JHP generated the STAT1 Tg mice and reviewed the manuscript. AVV and JJO performed the experiments, interpreted data, and wrote the manuscript. MS, HI, and RBH performed the experiments and reviewed the manuscript. TGM performed RNA-Seq data analysis and wrote the manuscript. HCL interpreted the data and critically reviewed the paper. MC contributed to design of the study, analyzed and interpreted the data, and wrote the manuscript.

Acknowledgments

We would like to thank the patients of the NIAID HIV Clinic for their participation in this study and the healthy controls of the NIH blood bank. We would like to thank Anthony Fauci (NIAID) for his guidance and support. We also would like to thank the NIAID Division of Intramural Research–operated (NIAID DIR–operated) Flow Cytometry Section for flow cytometric analyses and NIAID DIR–operated animal facilities for animal experiments and for their excellent technical assistance with mice. We thank NIAMS genomic facility, Francisco Otaizo-Carrasquero, and the NIAID Genomic Technologies Section facility. Computing systems support was provided by Bioinformatics and Molecular Analysis Section (CIT, NIH). This research was supported by the Intramural Research Program of the NIAID, NIH.

Address correspondence to: Marta Catalfamo, Department of Microbiology and Immunology, Georgetown University School of Medicine, 3970 Reservoir Road, N.W, New Research Building, Room EG19A, Washington, DC 20057, USA. Phone: 202.687.8675; Email: mc2151@georgetown.edu.

MC's present address is: Department of Microbiology and Immunology. Georgetown University School of Medicine, Washington DC, USA.

1. Boyman O, Purton JF, Surh CD, Sprent J. Cytokines and T-cell homeostasis. *Curr Opin Immunol*. 2007;19(3):320–326.
2. Tough DF, Sprent J. Turnover of naive- and memory-phenotype T cells. *J Exp Med*. 1994;179 (4):1127–1135.
3. Tan JT, et al. IL-7 is critical for homeostatic proliferation and survival of naive T cells. *Proc Natl Acad Sci USA*. 2001;98 (15):8732–8737.
4. Tan JT, Ernst B, Kieper WC, LeRoy E, Sprent J, Surh CD. Interleukin (IL)-15 and IL-7 jointly regulate homeostatic proliferation of

memory phenotype CD8+ cells but are not required for memory phenotype CD4+ cells. *J Exp Med*. 2002;195 (12):1523–1532.
5. Jacobs SR, Michalek RD, Rathmell JC. IL-7 is essential for homeostatic control of T cell metabolism in vivo. *J Immunol*. 2010;184 (7):3461–3469.
6. Tanchot C, Lemonnier FA, Pérarnau B, Freitas AA, Rocha B. Differential requirements for survival and proliferation of CD8 naive or memory T cells. *Science*. 1997;276(5321):2057–2062.
7. Kirberg J, Berns A, von Boehmer H. Peripheral T cell survival requires continual ligation of the T cell receptor to major histocompatibility complex-encoded molecules. *J Exp Med*. 1997;186 (8):1269–1275.
8. Goldrath AW, Bevan MJ. Low-affinity ligands for the TCR drive proliferation of mature CD8+ T cells in lymphopenic hosts. *Immunity*. 1999;11 (2):183–190.
9. Surh CD, Sprent J. Homeostasis of naive and memory T cells. *Immunity*. 2008;29(6):848–862.
10. Takada K, Jameson SC. Naive T cell homeostasis: from awareness of space to a sense of place. *Nat Rev Immunol*. 2009;9 (12):823–832.
11. Carrette F, Surh CD. IL-7 signaling and CD127 receptor regulation in the control of T cell homeostasis. *Semin Immunol*. 2012;24 (3):209–217.
12. Jameson SC, Lee YJ, Hogquist KA. Innate memory T cells. *Adv Immunol*. 2015;126:173–213.
13. Hakim FT, et al. Constraints on CD4 recovery postchemotherapy in adults: thymic insufficiency and apoptotic decline of expanded peripheral CD4 cells. *Blood*. 1997;90 (9):3789–3798.
14. Mackall CL, Hakim FT, Gress RE. Restoration of T-cell homeostasis after T-cell depletion. *Semin Immunol*. 1997;9 (6):339–346.
15. Douek DC. The contribution of the thymus to immune reconstitution after hematopoietic stem-cell transplantation. *Cytotherapy*. 2002;4 (5):425–426.
16. Catalfamo M, et al. HIV infection-associated immune activation occurs by two distinct pathways that differentially affect CD4 and CD8 T cells. *Proc Natl Acad Sci USA*. 2008;105 (50):19851–19856.
17. Vrisekoop N, et al. Restoration of the CD4 T cell compartment after long-term highly active antiretroviral therapy without phenotypical signs of accelerated immunological aging. *J Immunol*. 2008;181 (2):1573–1581.
18. Connors M, et al. HIV infection induces changes in CD4+ T-cell phenotype and depletions within the CD4+ T-cell repertoire that are not immediately restored by antiviral or immune-based therapies. *Nat Med*. 1997;3(5):533–540.
19. Gea-Banacloche JC, et al. Progression of human immunodeficiency virus disease is associated with increasing disruptions within the CD4+ T cell receptor repertoire. *J Infect Dis*. 1998;177 (3):579–585.
20. Foulds KE, Zenewicz LA, Shedlock DJ, Jiang J, Troy AE, Shen H. Cutting edge: CD4 and CD8 T cells are intrinsically different in their proliferative responses. *J Immunol*. 2002;168 (4):1528–1532.
21. Catalfamo M, Le Saout C, Lane HC. The role of cytokines in the pathogenesis and treatment of HIV infection. *Cytokine Growth Factor Rev*. 2012;23 (4-5):207–214.
22. Douek D. HIV disease progression: immune activation, microbes, and a leaky gut. *Top HIV Med*. 2007;15 (4):114–117.
23. Kovacs JA, et al. Identification of dynamically distinct subpopulations of T lymphocytes that are differentially affected by HIV. *J Exp Med*. 2001;194 (12):1731–1741.
24. Catalfamo M, et al. CD4 and CD8 T cell immune activation during chronic HIV infection: roles of homeostasis, HIV, type I IFN, and IL-7. *J Immunol*. 2011;186 (4):2106–2116.
25. Puel A, Ziegler SF, Buckley RH, Leonard WJ. Defective IL7R expression in T (-)B (+)NK (+) severe combined immunodeficiency. *Nat Genet*. 1998;20 (4):394–397.
26. Suzuki K, Nakajima H, Saito Y, Saito T, Leonard WJ, Iwamoto I. Janus kinase 3 (Jak3) is essential for common cytokine receptor gamma chain (gamma (c))-dependent signaling: comparative analysis of gamma (c), Jak3, and gamma (c) and Jak3 double-deficient mice. *Int Immunol*. 2000;12 (2):123–132.
27. Foxwell BM, Beadling C, Guschin D, Kerr I, Cantrell D. Interleukin-7 can induce the activation of Jak 1, Jak 3 and STAT 5 proteins in murine T cells. *Eur J Immunol*. 1995;25 (11):3041–3046.
28. Mazzucchelli R, Durum SK. Interleukin-7 receptor expression: intelligent design. *Nat Rev Immunol*. 2007;7 (2):144–154.
29. Jiang Q, et al. Cell biology of IL-7, a key lymphotrophin. *Cytokine Growth Factor Rev*. 2005;16 (4-5):513–533.
30. Min B, McHugh R, Sempowski GD, Mackall C, Foucras G, Paul WE. Neonates support lymphopenia-induced proliferation. *Immunity*. 2003;18 (1):131–140.
31. Swainson L, Kinet S, Mongellaz C, Sourisseau M, Henriques T, Taylor N. IL-7-induced proliferation of recent thymic emigrants requires activation of the PI3K pathway. *Blood*. 2007;109 (3):1034–1042.
32. Gil MP, et al. Regulating type 1 IFN effects in CD8 T cells during viral infections: changing STAT4 and STAT1 expression for function. *Blood*. 2012;120 (18):3718–3728.
33. Villarino AV, Kanno Y, Ferdinand JR, O'Shea JJ. Mechanisms of Jak/STAT signaling in immunity and disease. *J Immunol*. 2015;194 (1):21–27.
34. Jiang Q, et al. Distinct regions of the interleukin-7 receptor regulate different Bcl2 family members. *Mol Cell Biol*. 2004;24 (14):6501–6513.
35. Rochman I, Watanabe N, Arima K, Liu YJ, Leonard WJ. Cutting edge: direct action of thymic stromal lymphopoietin on activated human CD4+ T cells. *J Immunol*. 2007;178 (11):6720–6724.
36. Lu N, Wang YH, Wang YH, Arima K, Hanabuchi S, Liu YJ. TSLP and IL-7 use two different mechanisms to regulate human CD4+ T cell homeostasis. *J Exp Med*. 2009;206 (10):2111–2119.
37. Le Saout C, et al. Chronic exposure to type-I IFN under lymphopenic conditions alters CD4 T cell homeostasis. *PLoS Pathog*. 2014;10 (3):e1003976.
38. Min B, Yamane H, Hu-Li J, Paul WE. Spontaneous and homeostatic proliferation of CD4 T cells are regulated by different mechanisms. *J Immunol*. 2005;174 (10):6039–6044.
39. Schluns KS, Kieper WC, Jameson SC, Lefrançois L. Interleukin-7 mediates the homeostasis of naive and memory CD8 T cells in vivo. *Nat Immunol*. 2000;1 (5):426–432.
40. Asquith B, Borghans JA, Ganusov VV, Macallan DC. Lymphocyte kinetics in health and disease. *Trends Immunol*. 2009;30 (4):182–189.

41. Chomont N, et al. HIV reservoir size and persistence are driven by T cell survival and homeostatic proliferation. *Nat Med*. 2009;15 (8):893–900.
42. Vandergeeten C, et al. Interleukin-7 promotes HIV persistence during antiretroviral therapy. *Blood*. 2013;121 (21):4321–4329.
43. Sammicheli S, et al. IL-7 promotes CD95-induced apoptosis in B cells via the IFN-γ/STAT1 pathway. *PLoS ONE*. 2011;6 (12):e28629.
44. Kimura MY, et al. IL-7 signaling must be intermittent, not continuous, during $CD8^+$ T cell homeostasis to promote cell survival instead of cell death. *Nat Immunol*. 2013;14 (2):143–151.
45. Lee CK, Smith E, Gimeno R, Gertner R, Levy DE. STAT1 affects lymphocyte survival and proliferation partially independent of its role downstream of IFN-gamma. *J Immunol*. 2000;164 (3):1286–1292.
46. Nguyen TP, et al. Interferon-α inhibits CD4 T cell responses to interleukin-7 and interleukin-2 and selectively interferes with Akt signaling. *J Leukoc Biol*. 2015;97 (6):1139–1146.
47. Plumb AW, et al. Interleukin-7, but not thymic stromal lymphopoietin, plays a key role in the T cell response to influenza A virus. *PLoS ONE*. 2012;7(11):e50199.
48. Pellegrini M, et al. IL-7 engages multiple mechanisms to overcome chronic viral infection and limit organ pathology. *Cell*. 2011;144 (4):601–613.
49. Feng CG, Zheng L, Lenardo MJ, Sher A. Interferon-inducible immunity-related GTPase Irgm1 regulates IFN gamma-dependent host defense, lymphocyte survival and autophagy. *Autophagy*. 2009;5 (2):232–234.
50. De Rosa SC, Herzenberg LA, Herzenberg LA, Roederer M. 11-color, 13-parameter flow cytometry: identification of human naive T cells by phenotype, function, and T-cell receptor diversity. *Nat Med*. 2001;7 (2):245–248.
51. Subramanian A, et al. Gene set enrichment analysis: a knowledge-based approach for interpreting genome-wide expression profiles. *Proc Natl Acad Sci USA*. 2005;102 (43):15545–15550.
52. Park JH, et al. Suppression of IL7Ralpha transcription by IL-7 and other prosurvival cytokines: a novel mechanism for maximizing IL-7-dependent T cell survival. Immunity. 2004;21(2):289–302.